References

1. J. G. PERKINS and P. T. STROUD, AWRE Report No. 09/70 (January 1970).
2. P. T. STROUD, J. G. PERKINS, L. E. COLLINS and K. G. STEPHENS, Nuclear Res. Note 14/71 SSNR AWRE (April 1971).
3. J. G. PERKINS and P. T. STROUD, *Nuclear Instrum. and Methods* 102 (1972) 109.

Received 9 September and accepted 4 October 1976

J. S. COLLIGON
G. FISCHER
M. H. PATEL
Department of Electrical Engineering, University of Salford, Lancs, UK

Fracture energy of plain and glass-reinforced gypsum plaster

Recent work from this laboratory [1, 2] has clearly demonstrated that addition of a small amount of glass fibre to gypsum plaster converts this essentially brittle material into a quasi-ductile one. This is manifested in the high impact strength of the composite, which is far superior to that of the unreinforced plaster if measured by the pendulum (Izod or Charpy) or the dropping weight methods. Several applications where this improved toughness of glass-reinforced gypsum (grg) can be gainfully utilized have already been suggested [3]. The tests mentioned above, however, do not offer any insight into the processes attending impact failures and for obtaining such information it is sometimes rewarding to consider an approach based on fracture mechanics. For brittle matrix composites such as those based on ceramics, cements or glass, such fracture mechanics studies have already produced some useful results [4–6]. In the present work, similar information has been gathered for gypsum plaster and grg by determining the critical strain energy release rates (G_{IC}) for these materials and their average surface work of fracture (γ_F). γ_F, defined here as the work done to create unit area of new fracture face not taking into account fine scale irregularities in the fracture face, was measured following the techniques developed by Nakayama [7] and Tattersall and Tappin [8]. Phillips [6] has recently discussed the relevance of these measurements for brittle matrix composites.

The gypsum plaster used was fine casting plaster supplied by a UK manufacturer and conforming to BS 1191, Part 1, Class A category. A retarder was added to the plaster at the time of the preparation of the slurry. Slurries having water/plaster ratios (W/P) in the range 0.5 to 0.33 were poured into moulds and after the material had hardened, it was demoulded and test specimens cut from it. The lowest W/P ratio was obtained by removing the excess water by applying suction to the base of the mould.

Glass fibre-reinforced gypsum (grg) was prepared by the spray-suction technique developed at BRE [1, 3]. In this method, glass-fibre strands chopped to suitable lengths assume a random two-dimensional distribution in the plane of the mould. In the present work, the grg boards contained approximately 5 vol% of 32 mm long glass fibres. The glass-fibre strands consisted of 204 filaments of 9.5 μm diameter. Plaster from the same batch used in the manufacture of grg was also cast into moulds at the same time to provide control specimens. The W/P ratio of the "wet" board after suction was 0.33.

In addition to the parameters G_{IC} and γ_F, the bending and impact strength of both plain and reinforced plaster were also determined. For all tests, specimens were cut in the form of rectangular beams of nominal cross-section 10 mm × 17 mm and length 130 mm. One batch of specimens had a larger cross-sectional area, 18 mm × 17 mm. Charpy impact tests were carried out with specimens 75 mm long.

In some of the beams cracks were simulated by cutting central slits with a fine saw, 0.2 mm thick. In some cases the tip of the saw-cut was sharpened with a razor blade. For plain plaster, crack length to beam depth ratios, c/d, were varied initially in the range 0.1 to 0.8, to examine the validity of the fracture mechanics approach in this particular case. For later specimens, prepared with different W/P ratios, only one c/d (0.48) was used. Notched grg specimens were prepared with a c/d ratio of 0.43.

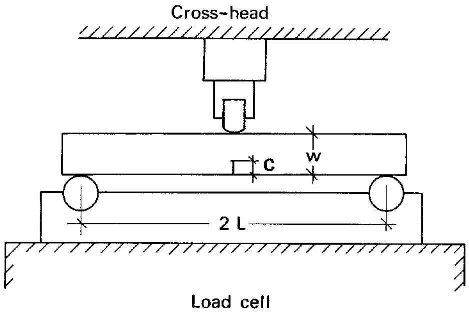

Figure 1 Specimen geometry and loading arrangement.

Beams of plain plaster and grg were deformed in three-point bending (Fig. 1) on an Instron universal testing machine using a load cell of spring constant $4 \times 10^7 \text{N m}^{-1}$ and a cross-head speed of 0.5mm min^{-1}. The entire load deflection curves (Figs. 2 and 3) were recorded and a mechanical integrator attached to the Instron measured the work done on the specimen during the test. The estimates of the average work of fracture (γ_F) were made by dividing these measured values by the cross-sectional area of both fracture faces. The modulus of rupture (MOR) and the stress at the limit of proportionality (LOP) were calculated

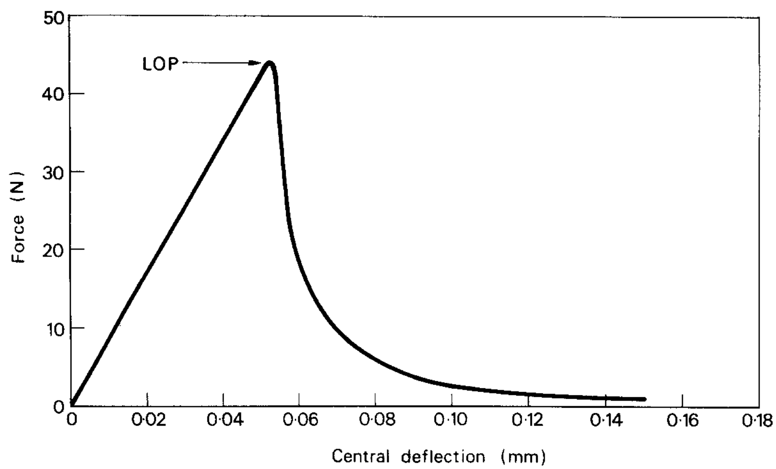

Figure 2 Force–deflection curve of stable fracture in notched plaster specimens.

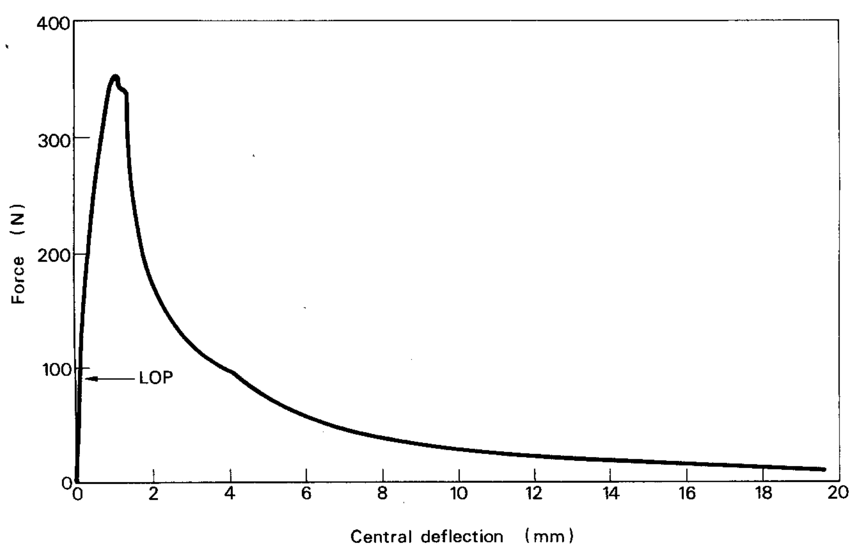

Figure 3 Force–deflection curve for grg notched specimens.

from loads at failure and at the LOP respectively using unnotched specimens and elastic beam theory.

Following Brown and Strawley [9], the critical strain energy release rate (G_{IC}) can be written as

$$G_{IC} = \frac{9P^2L^2c}{Eb^2d^4}y^2 \qquad (1)$$

where P = critical load, L = moment arm (half span), c = crack length, E = Young's modulus, b = beam breadth and d = beam depth; y is a polynomial in c/d and its value depends on specimen geometry. The critical load refers to the load at which the crack begins to extend. The extension of the crack is accompanied by a reduction in the stiffness of the specimen which is observed as a departure from linearity on the load displacement curve. The load at this point (LOP) was used in the calculation of G_{IC} in the present work.

The LOP could be easily located in the case of plain plaster specimens as it virtually coincided with the ultimate load reached (Fig. 2). The load–deflection plots of grg, on the other hand, showed only a gradual change in slope and it was not possible to locate with any degree of certainty, the points where the curves started to deviate from linearity. The position of the LOP in this case was taken to be the point where the smallest departure from linearity could be detected. For the recording system used in this study, the magnitude of this quantity was 0.8% of the secant modulus.

Specimens of plain plaster prepared with W/P ratios 0.42 to 0.54 were tested as shallow beams with the short dimension as the depth. All other specimens were tested as deep beams with the larger dimension as the depth. The values of y in Equation 1 corresponding to these two specimen configurations are respectively:

$$y = 1.96 - 2.75\left(\frac{c}{d}\right) + 13.66\left(\frac{c}{d}\right)^2 - 23.98\left(\frac{c}{d}\right)^3 + 25.22\left(\frac{c}{d}\right)^4$$

and

$$y = 1.95 - 2.91\left(\frac{c}{d}\right) + 14.1\left(\frac{c}{d}\right)^2 - 24.55\left(\frac{c}{d}\right)^3 + 25.51\left(\frac{c}{d}\right)^4.$$

The impact strength of the materials under investigation was measured on a Charpy type impact machine. The grg was tested with the machine set to its maximum energy of 16.3 J and a striking velocity of 3.48 m sec^{-1}. For the plain plaster, the swing of the pendulum was much reduced so that its energy was little more than required to break the specimen. The initial energy and striking velocity for the notched and unnotched specimens were, respectively, 12×10^{-3} J, 0.09 m sec^{-1} and 77×10^{-3} J and 0.23 m sec^{-1}.

Table I lists the values of G_{IC} and $2\gamma_F$ obtained with plain plaster for a range of c/d values. Because of the difference in the conventional definition of work of fracture and strain energy release rate, G_{IC} values are compared with $2\gamma_F$. Within the central range of c/d ratios, 0.25 to 0.60, the strain energy release rate was fairly constant giving an average value of 13.7 J m^{-2} while $2\gamma_F$ fell somewhat from 19.4 to 16.4 J m^{-2}. For shallower notches fracture was unstable and both G_{IC} and $2\gamma_F$ showed a marked increase; for deeper notches they decreased. Sharpening the tip of the sawn notch with a razor blade or doubling the width of the beam had little effect on the magnitude of these parameters.

Table II shows the results obtained with plain plaster for a range of W/P ratios. All the notched beams ($c/d = 0.48$) fractured in a stable manner and thus $2\gamma_F$ may be taken to represent the average energy required to form the new surfaces. This was consistently about 4 J m^{-2} higher than the G_{IC} values.

The effect of adding ~5% of glass fibres

TABLE I Properties of gypsum plaster with a range of c/d ratios, W/P = 0.33, E = 14.81 GN m^{-2}. S.D. shown in brackets

c/d	G_{IC} (J m^{-2})	$2\gamma_F$ (J m^{-2})	Remarks
0.115	15.94 (1.02)	26.07 (1.79)	unstable fracture
0.194	16.46 (3.90)	24.22 (2.91)	semi-stable fracture
0.256	13.32 (3.13)	19.40 (1.93)	razor cut
0.360	13.61 (3.46)	18.75 (1.07)	
0.468	13.60 (3.63)	18.00 (0.33)	
0.495	14.88 (1.25)	17.62 (0.59)	double width specimen
0.583	13.89 (2.62)	17.30 (0.89)	razor cut
0.596	12.93 (1.95)	16.42 (0.50)	
0.688	7.59 (1.10)	13.60 (1.47)	
0.698	5.41 (0.95)	12.42 (0.95)	razor cut
0.793	7.47 (2.54)	13.40 (1.44)	

TABLE II Properties of gypsum plaster with a range of W/P ratios. S.D. shown in brackets

W/P	Density ($g\,cm^{-3}$)	E ($GN\,m^{-2}$)	LOP stress ($MN\,m^{-2}$)	G_{IC} ($J\,m^{-2}$)	$2\gamma_F$ ($J\,m^{-2}$)
0.54	1.27	7.89	6.58	5.33 (0.28)	9.50 (0.56)
0.50	1.32	8.69	7.24	5.70 (0.35)	10.21 (0.34)
0.46	1.39	9.55	8.03	6.52 (0.46)	10.50 (0.81)
0.42	1.47	11.24	7.93	6.87 (0.59)	11.21 (0.74)
0.33	1.62	14.81	11.79	13.63 (3.63)	17.62 (0.33)

(32 mm long strands in a two-dimensional arrangement) to gypsum plaster is shown in Table III where the results are compared with control samples containing no glass. Each value represents an average of 9 or 10 specimens. It is seen that as a result of glass addition, G_{IC} was increased by a factor of 4 and $2\gamma_F$ by a factor of 750, for the notched specimens. Notching of the specimen did not have much effect on the $2\gamma_F$ values of the composite specimens since fracture was always stable. The same was found to be the case for the results of the Charpy impact tests. Unnotched plain plaster specimens exhibited unstable fracture and hence gave large $2\gamma_F$ and Charpy values (Table III).

Table III also gives the size of the inherent edge crack in the unnotched specimens. This was determined by inserting the measured values of G_{IC} and stress at the LOP in Equation 1 and solving for c. The presence of the fibres has caused an increase in the inherent value of c from 0.33 to 0.93 mm.

This work has clearly demonstrated that addition of glass fibres to gypsum plaster produces a composite material with a very high value for the work of fracture and a significantly improved "apparent fracture toughness" [5] *vis à vis* that of the matrix.

Unnotched specimens of plain plaster fail catastrophically. The measured values of $2\gamma_F$ then represent the elastic energy stored during the test and thus depends on specimen geometry and the stiffness of the loading frame. With notched specimens, it was possible to obtain stable fracture for a range of c/d ratios and the value of $2\gamma_F$ obtained in these cases, $\sim 17\,J\,m^{-2}$ (Table I) may be taken as the material property for gypsum plaster prepared with a water/plaster ratio of 0.33. At higher W/P ratios the decrease in $2\gamma_F$ results from the lowering of strength and stiffness of plaster samples due to increased porosity [2].

The average work of fracture values for grg was found to be higher by several orders of magnitude than those of the unreinforced material, in agreement with the observations made by other investigators on similar materials [10, 11]. The values of $2\gamma_F$ are similar for plain and notched specimens of grg as the presence of fibres ensures a stable fracture even in unnotched specimens.

The Charpy test results also demonstrate the superior impact strength of grg. These estimates are higher than the corresponding $2\gamma_F$ values but the reasons for this difference are not entirely clear. Similar differences have been recorded for fibre cement composites by Briggs *et al.* [12].

TABLE III Properties of glass fibre-reinforced gypsum plaster and plain gypsum plaster. S.D. shown in brackets

	Unnotched samples		Notched samples	
	grg	Gypsum plaster	grg	Gypsum plaster
c/d ratio	–	–	0.429	0.420
Density ($g\,cm^{-3}$)	1.67 (0.03)	1.65 (0.02)	1.67 (0.03)	1.65 (0.02)
E ($GN\,m^{-2}$)	16.4 (0.43)	15.8 (0.72)	16.4 (0.43)	15.8 (0.72)
MOR ($MN\,m^{-2}$)	45.3 (1.81)	12.0 (1.01)	–	–
LOP stress ($MN\,m^{-2}$)	14.8 (1.42)	12.0 (1.01)	–	–
G_{IC} ($J\,m^{-2}$)	–	–	43.4 (34.9)	10.8 (1.25)
$2\gamma_F$ ($J\,m^{-2}$)	13600 (1710)	88.5 (15.0)	13200. (1170)	17.6 (0.91)
Charpy ($J\,m^{-2}$)	30400 (2460)	391 (92.6)	30600 (2240)	87.4 (26.6)
Inherent edge notch (mm)	0.93	0.33	–	–

The critical strain energy release rates for plaster and grg specimens were determined from the experimental values of the load at the LOP (Figs. 2 and 3). It is quite clear, particularly from Fig. 3, that following the LOP there is a determinable region of non-elastic behaviour before significant movements of cracks take place in the material. One reason for the existence of this region could be plastic deformation of the material at the crack-tip. In the present study a detailed examination of this phenomenon was not made and it was assumed that the material behaved elastically up to the LOP, and the corresponding G_{IC} values represented fracture energies at crack initiation.

Like γ_F, G_{IC} values of plain plaster decreased with an increase in the W/P ratio (i.e. decrease in density). For G_{IC} values of grg it should be noted (Table III) that there was considerable scatter in the data, the lowest value being similar to that of plain plaster and the highest $106\,J\,m^{-2}$. This variability illustrates the difficulty encountered in measuring even the "apparent" fracture toughness of fibre composites. It is likely that in those cases where the G_{IC} values are low, fibres are not present in the proximity of the notch whereas high G_{IC} values reflect an untypical concentration of fibres near the root of the notch. In this respect the zone over which the fibres exert their influence remains unknown but the effect of fibre addition on G_{IC} values of plaster is so large that one may speculate that cracking of the matrix is restrained by the fibres. Such a conclusion has been reached by several investigators recently, arguing from different viewpoints [13, 14].

It is also seen from Table III that the length of the inherent edge crack in grg is three times that of plain plaster. The stresses at the LOP for these two materials are not very different. If the inherent edge crack of the composite could be reduced without changing the G_{IC} value very much, there is the prospect of increasing the stress at the LOP substantially. This may possibly be achieved by selecting the appropriate diameter for the fibre reinforcement.

It has been seen, therefore, that when glass fibres are added to a brittle matrix like gypsum plaster, the critical strain energy release rate and the average surface work of fracture of the unreinforced material are greatly increased. For plain plaster both these properties depend on the proportion of water used in the preparation of the material, increasing as the water/plaster ratio is decreased. This is due to the higher strength and stiffness of plaster at relatively higher density.

At 5 vol % addition of 32 mm glass-fibre strands in random two-dimensional orientation, G_{IC}, $2\gamma_F$ and Charpy impact strength values of glass-reinforced gypsum were, respectively, 4, 750 and 350 times those of the unreinforced matrix when notched specimens were used. These properties make grg not a brittle but a quasi-ductile material.

Acknowledgement
The work described has been carried out as part of the research programme of the Building Research Establishment of the Department of the Environment and this paper is published by permission of the Director.

References
1. M. A. ALI and F. J. GRIMER, *J. Mater. Sci.* 4 (1969) 389.
2. M. A. ALI and B. SINGH, *ibid* **10** (1975) 1920.
3. J. F. RYDER, 'Prospects for fibre reinforced construction materials'. Conf. pro. of International Building Exhibition (BRS 1971).
4. R. W. DAVIDGE, in 'Fracture mechanics of ceramics', Vol. 2, edited by R. C. BRADT, D. P. H. HASSELMAN and F. F. LANGE (Plenum, New York, 1974).
5. J. H. BROWN, *Mag. Concr. Res.* **25** (1973) 31.
6. D. C. PHILLIPS, *J. Mater. Sci.* 9 (1974) 1847.
7. J. NAKAYAMA, *J. Amer. Ceram. Soc.* **48** (1965) 583.
8. H. G. TATTERSALL and G. TAPPIN, *J. Mater. Sci.* **1** (1966) 296.
9. W. F. BROWN and J. E. STRAWLEY, ASTM Spec. Pub. 410, Philadelphia (1966).
10. B. HARRIS, J. VARLOW, and C. D. ELLIS, *Cem. Concr. Res.* 2 (1972) 447.
11. J. C. ALESZKA and P. W. R. BEAUMONT, "Polymers in concrete", Conference Proceedings of the First International Congress on Polymer Concretes (Construction Press Ltd, Lancaster, UK, 1976).
12. A. BRIGGS, D. H. BOWEN, and J. KOLLEK, "Carbon fibres, their place in modern technology", Conference Proceedings of the 2nd International Carbon Fibre Conference (The Plastics Institute, London, 1974).

13. J. P. ROMUALDI, and G. B. BATSON, *Proc. Amer. Soc. Civil Engineer* 89 EM3 (1963) 147.
14. J. AVESTON, G. A. COOPER and A. KELLY, "The properties of fibre composites", Proceedings of a Conference at National Physical Laboratory (IPC, London, 1972).

*Received 6 October
and accepted 8 November 1976*

P. L. WALTON
A. J. MAJUMDAR
*Building Research Establishment,
Building Research Station,
Garston,
Watford, UK*

The pressure–temperature phase diagrams of the HgTe and $Hg_{1-x}Cd_xTe$ systems

The use of $Hg_{1-x}Cd_xTe$ alloys to produce solid state devices capable of detecting radiation in the infrared ranges is well established. In the production of material which is suitable for device manufacture it has been found necessary to anneal some of the as-grown crystals in suitable Hg-rich atmospheres to achieve the correct electrical properties [1]. Thus, for photoconductive devices which will operate in the 10 to 14 μm range at 77 K, n-type material with carrier concentrations of $5 \times 10^{14}\,\mathrm{cm}^{-3}$ and Hall mobilities of $2 \times 10^5\,\mathrm{cm^2\,V^{-1}\,sec^{-1}}$ are required, whereas photovoltaic detectors require a p-type substrate with carrier concentrations of $\sim 10^{17}\,\mathrm{cm}^{-3}$.

Although several workers [2, 3, 7] have studied the closely similar pressure–temperature diagrams for both the binary and ternary systems, there still appears to be considerable disagreement concerning the position of the $p \rightleftharpoons n$ intrinsic–extrinsic lines for these materials. It is, therefore, essential to define this transition more closely in order to obtain the correct electrical properties reproducibly.

In an attempt to clarify this situation a series of single and two temperature annealing experiments have been carried out with as-grown materials obtained from both the Bridgman and cast-recrystallization growth techniques. The results of these studies together with a summary of the earlier work on these materials is presented in Fig. 1.

In the case of the binary HgTe system, it would appear that the original intrinsic–extrinsic line proposed by Rodot [4] is still generally valid, although its position at high mercury pressures is somewhat uncertain as the results of Strauss and Brebrick [2] suggest that p-type material can be obtained at temperatures lower than those predicted by Rodot.

The results for the pseudo-binary $Hg_{1-x}Cd_xTe$ system in the range x Cd 0.12 to 0.22 suggest that the original proposition by Schmit and Speerschneider [3] needs some modification. The present results taken with the earlier ones do not allow us to define the intrinsic–extrinsic line exactly and it is best represented by a band as indicated in Fig. 1. It should be noted that the line proposed by Schmit and Speerschneider represents a high-temperature boundary to the band.

Considering the range of existence of p- and n-type materials, it is apparent that $Hg_{1-x}Cd_xTe$ $(0.12 < x < 0.22)$ is n-type below 400 to 450° C and 260 to 280° C on the mercury and tellurium saturated solidii, respectively.

Although the precise values of the carrier concentrations will depend upon the exact thermal and crystallographic histories of the specimens, an indication of the mean values which can be expected is given for materials which have been annealed at the temperatures–pressure combinations shown in Fig. 1.

An exact defect model is still needed to explain these intrinsic to extrinsic changes in the binary and ternary systems; however, the present authors suspect that the instabilities which may occur in the sphalerite structure in the ternary system [10] will contribute to the nature of the defects at higher temperatures and mercury pressures.

Acknowledgement
The authors gratefully acknowledge the support provided for this programme by the Ministry of Defence, Procurement Executive, D.C.V.D.

References
1. J. NISHIZAWA, K. SUTO, M. KITAMURA, M. SATO, Y. TAKASE and A. ITO, *J. Phys. Chem. Solids* 37 (1976) 33.